A computational platform for seismic performance assessment of reinforced concrete bridge piers with unbonded reinforcing or prestressing bars

T.-H. Kim[1], J.-G. Park[2], Y.-J. Kim[1] and H. M. Shin[*2]

*[1]Civil Engineering Research Team, Daewoo Institute of Construction Technology,
60 Songjuk-dong, Jangan-gu, Suwon, Kyonggi-do, 440-210, Korea
[2]Department of Civil and Environmental Engineering, Sungkyunkwan University,
300 Chunchun-dong, Jangan-gu, Suwon, Kyonggi-do, 440-746, Korea*

Abstract.   This paper presents a nonlinear finite element analysis procedure for the seismic performance assessment of reinforced concrete bridge piers with unbonded reinforcing or prestressing bars. A computer program named RCAHEST (Reinforced Concrete Analysis in Higher Evaluation System Technology) is used to analyze reinforced concrete structures; this program was also used in our study. Tensile, compressive and shear models of cracked concrete and models of reinforcing and prestressing steel were used account for material nonlinearity of reinforced concrete. The smeared crack approach was incorporated. To represent the interaction between unbonded reinforcing or prestressing bar and concrete, an unbonded reinforcing or prestressing bar element based on the finite element method was developed in this study. The proposed numerical method for the seismic performance assessment of reinforced concrete bridge piers with unbonded reinforcing or prestressing bars is verified by comparison of its results with reliable experimental results.

Keywords: seismic performance; reinforced concrete bridge piers; unbonded reinforcing or prestressing bars; material nonlinearity; finite element method.

1. Introduction

Energy dissipation capacities of reinforced concrete bridge piers during earthquake excitation can be increased by confining the plastic hinge regions, which would ensure high values of ductility factor. However, during previous earthquakes, residual displacements of large magnitude were observed, despite high-energy dissipation capacities. High residual displacements may prevent both serviceability and damage recovery of the bridge piers after the earthquakes.

With respect to the mechanical behavior of bridge piers with vertical prestressing, various research (Ito, *et al.* 1997, Kwan and Billington 2001) has clarified and confirmed that a bridge pier's ability for restoration can eliminate residual deformation after severe earthquakes (see Fig. 1).

In recent years, reinforced concrete bridge piers with unbonded prestressing bars have been studied and designed because of their excellent mechanical characteristics and their practical advantages in construction. However, actual bridge piers with vertical prestressing, have some problems such as construction cost and inadequate vertical prestressing methods (Ikeda, *et al.* 2002,

---

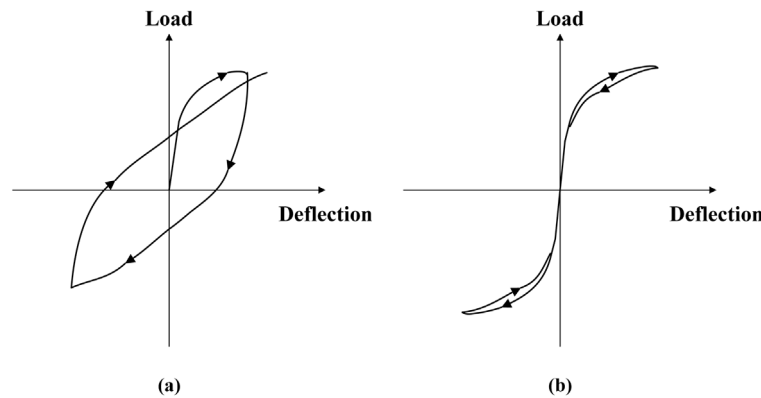* Corresponding Author, E-mail: hmshin@skku.ac.kr

Fig. 1 Schematic hysteretic response: (a) structural system with bonded bar; (b) structural system unbonded
    bar

Mori, *et al.* 2002).

   Prestressed concrete members exhibit stable seismic performance under a combined action of shear and flexure. Therefore, the flexure and shear capacities of reinforced concrete bridge piers with unbonded prestressing bars are expected to be better than those of standard reinforced concrete bridge piers. Construction periods may be reduced by using pre-cast concrete segments. However, reinforced concrete bridge piers with unbonded prestressing bars have been seldom constructed throughout the world in spite of their merits, most likely because of the lack of experience in construction and possible cost increase. Sometimes, reinforced concrete bridge piers with unbonded prestressing bars may dissipate less energy because than the standard reinforced concrete bridge piers because the former has fewer concrete cracks (Mutsuyoshi, *et al.* 2001).

   To find alternative methods of handling this issue without the conventional reliance on shear reinforcement alone, the enhancement of seismic performance of reinforced concrete bridge piers with respect to shear strength and ductility by controlling the bond of longitudinal reinforcements was investigated (Pandey and Mutsuyoshi 2004).

   In a reinforced concrete bridge pier, the longitudinal bars are damaged by local buckling and rupture in the plastic hinge under extreme earthquake excitation (Chung, *et al*. 2004). One of the measures used to mitigate such concentrated damage to the longitudinal bars is to unbond the longitudinal bars from the concrete at the plastic hinge (see Fig. 2). When the longitudinal bar is unbonded to the concrete, the stress distribution inside the concrete changes dramatically. This stress condition frees the whole shear span from cracks, and thus, effectively prevents diagonal shear failure, which can eventually enhance the shear performance of bridge piers (Ranasinghe, *et al.* 2002).

   The main purposes of this study are to investigate the possible enhancement of seismic performance of reinforced concrete bridge piers with unbonded reinforcing or prestressing longitudinal bars with respect to shear strength and ductility and to analyze the seismic response behavior of reinforced concrete bridge piers with unbonded longitudinal bars.

   An evaluation method for the seismic performance of reinforced concrete bridge piers with unbonded reinforcing or prestressing bars is proposed by using and modifying a nonlinear finite element analysis program (RCAHEST, Reinforced Concrete Analysis in Higher Evaluation System Technology), developed by the authors (Kim and Shin 2001, Kim, *et al.* 2002, Kim, *et al.* 2003, Kim, *et al.* 2005). To represent the interaction between unbonded reinforcing or prestressing bar and

Bonded column   **Unbonded column**

Cracks and
spalling of
concrete

Few cracks due to
averaging stain over
the unbonded zone

Unbonded zone

Tension side : Few spalling of concrete
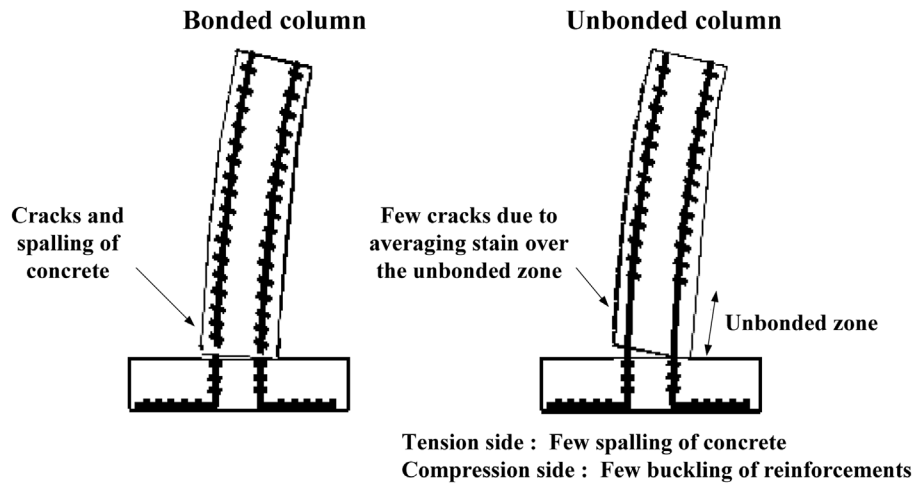**Compression side : Few buckling of reinforcements**

Fig. 2 Effect of unbonded reinforcing bars

concrete, an unbonded reinforcing or prestressing bar element is newly developed and this element is added to the element library of RCAHEST in this study.

To assess the program RCAHEST with respect to its ability to predict the seismic performance of reinforced concrete bridge piers with unbonded reinforcing or prestressing bars, the program's results were compared with the results of various experimental tests.

2. Nonlinear finite element analysis program RCAHEST

RCAHEST is a nonlinear finite element analysis program for analyzing reinforced concrete structures. The program has been developed by Kim and Shin (2001), at the Department of Civil and Environmental Engineering, Sungkyunkwan University.

The proposed structural element library of RCAHEST is built around the finite element analysis program shell named FEAP, developed by Taylor (2000). FEAP is characterized by modular architecture and by the facility that is used to introduce the type of custom elements, input utilities, and custom strategies and procedures.

The elements developed for the inelastic finite element analyses of reinforced concrete bridge piers under earthquake excitation are a reinforced concrete plane stress element and an interface element. The material models, described in the next sections, are used as stress-strain relations at Gauss integration points of each element.

Accompanying the present study, the authors attempt to implement such reinforced concrete plane stress element, interface element, and unbonded reinforcing or prestressing bar element which is newly developed to represent the interaction between unbonded reinforcing or prestressing bar and concrete as shown in Fig. 3, and to modify the material models in order to be suited to the seismic performance assessment.

2D or 3D Spring element	4 nodes PSC shell element	2D or 3D Flexibility-based fiber beam-column element	4 nodes Elastic shell element
Joint element	FEAP		4 nodes RC shell element
Unbonded reinforcing or prestressing bar element	Interface element	RC plane stress element	2D Elasto-plastic plane stress element

Fig. 3 Element library of RCAHEST

2.1. Nonlinear material model for reinforced concrete

The nonlinear material model for the reinforced concrete consists of models for concrete and a model for the reinforcing bars. Models for concrete may be divided into models for uncracked concrete and cracked concrete. The basic and widely-known model adopted for crack representation is based on the non-orthogonal fixed-crack method of the smeared crack concept. The approach using this model is practical for cyclic loads whose history needs to be recorded.

This section includes summaries of the material models used in the analysis. A full description of the nonlinear material model for reinforced concrete is given by Kim *et al.* (Kim and Shin 2001, Kim, *et al.* 2002, Kim, *et al.* 2003, Kim, *et al.* 2005).

2.1.1. Model for uncracked and cracked concrete

The widely used elasto-plastic and fracture model for the biaxial state of stress proposed by Maekawa and Okamura (1983) is used as the constitutive equation for uncracked concrete. For uncracked concrete, the nonlinearity, anisotropy, and strain softening effects are expressed independently of the loading history.

For cracked concrete, the three models are for depicting the behavior of concrete in the direction normal to the crack plane, in the direction of the crack plane, and in shear direction at the crack plane (see Fig. 4). Each constitutive model for cracked reinforced concrete element is formulated in the direction of orthogonal anisotropy.

Cracked concrete may resist a certain amount of tensile stress normal to the cracked plane because of the bond effect between the concrete and the reinforcing bars. A refined tension stiffening model is obtained by transforming the tensile stresses of concrete into the component normal to the crack, and improved accuracy is expected, especially when the reinforcing ratios in the orthogonal directions are significantly different and when the reinforcing bars are distributed only in one direction. For the tension stiffening model for unloading and reloading, the model proposed by Shima, *et al.* (1987) is basically used.
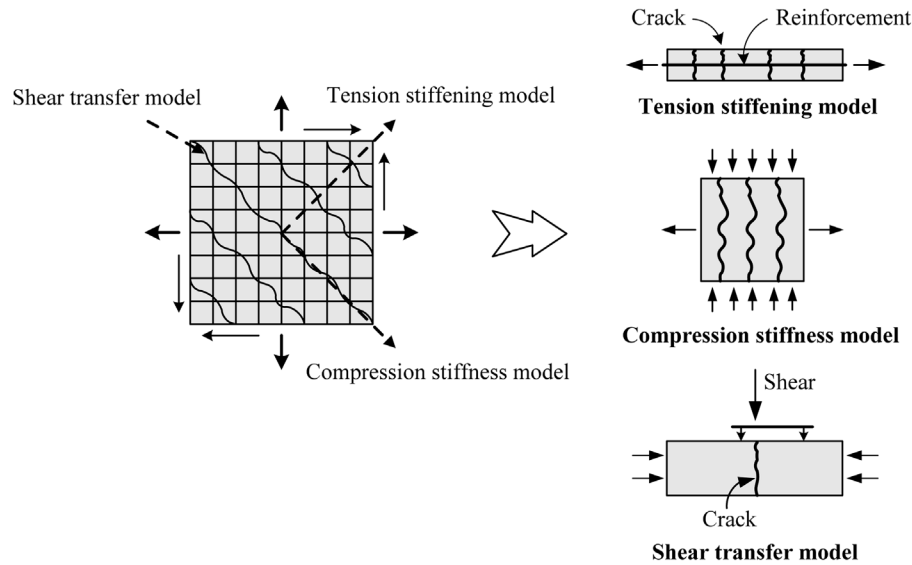
Fig. 4 Construction of cracked concrete model

A modified elasto-plastic fracture model is used to describe the compressive behavior of concrete struts in between cracks in the direction of the crack plane. The model describes the degradation in compressive stiffness by modifying the fracture parameter in terms of the strain perpendicular to the crack plane. The cyclic load causes damage to the inner concrete and energy is dissipated during the unloading and reloading processes. This behavior is considered in the model by modifying the stress-strain curve at unloading to an experimentally fitted quadratic curve.

The shear transfer model based on the contact surface density function (Li, *et al.* 1989) is used to consider the effect of shear stress transfer due to the aggregate interlock at the crack surface. The contact surface is assumed to respond elasto-plastically and the model is applicable to any arbitrary loading history. For the shear transfer model for unloading and reloading, the model modified by the authors is used.

2.1.2. Model for the reinforcing bars in concrete

The stress acting on the reinforcing bar embedded in concrete is not uniform and the stress value is the maximum at locations where the bar is exposed to a crack plane. The constitutive equations for the bare bar may be used if the stress strain relation is in the elastic range. The post-yield constitutive law for the reinforcing bar in concrete considers the bond characteristics and the model is a bilinear model as shown in Fig 5. Kato's model (1979) for the bare bar under the reversed cyclic loading and the assumption of a cosinusoidal stress distribution were used to derive the mechanical behavior of reinforcing bars in concrete under reversed cyclic loading.

For reinforcing bars under extreme compression, lateral bar buckling tends to occur, which greatly affects the post peak behavior and member ductility. To account for buckling of reinforcing bars, the average stress-strain behavior after concrete crushing is assumed to be linearly descending until the 20% average steel stress is reached (Kim, *et al.* 2005).
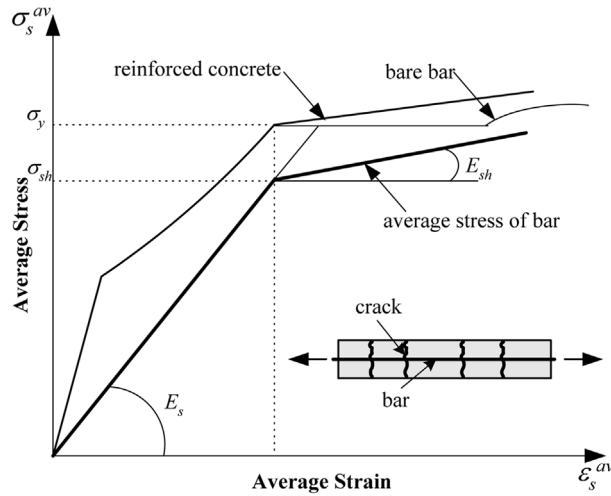
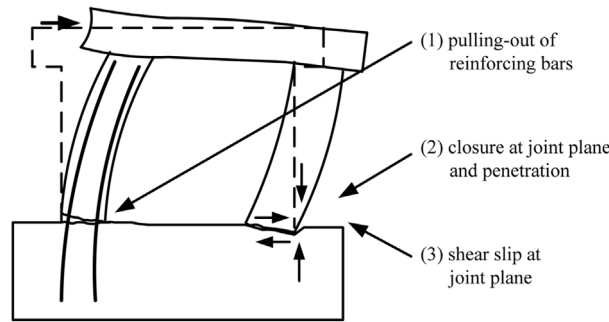Fig. 5 Model for reinforcing bar in concrete

Fig. 6 Three types of localized discontinuous deformation at boundary plane

2.1.3. Model and assumption for the interface

The local discontinuous deformation, which is a part of the anchorage slip, shear slip at the joint plane, and penetration at the joint plane, occurs according to the stiffness changing rapidly in the column and foundation etc. (see Fig. 6). Therefore, to accurately predict the response of the structures at the boundary plane, an interface element is required.

The interface model for the boundary plane connecting two reinforced concrete elements with different sections is based on the discrete crack concept, which uses the relationships between the stress and the localized deformations. The model is one-dimensional and has no thickness (see Fig. 7).

2.1.4. Model for fatigue damage

Fatigue damage of reinforced concrete bridge piers subjected to seismic load seems inevitable. Fatigue damage influencing the inelastic behavior of reinforced concrete bridge piers may be characterized as concrete strength deterioration and low cycle fatigue of reinforcing bars.

The formula of Kakuta, *et al.* (1982) derived from plain concrete specimen tests is adopted for the fatigue model of concrete. The formula is modified so that it can be applied to reinforced concrete (Kim, *et al.* 2005).

Reinforcing bars dominate the behavior of reinforced concrete members under seismic load. The

$$\delta_A = \delta_{(h)}^{actual} = \delta_{(h)}^{2-d} + \delta_{(h_i)}^{2-d}$$
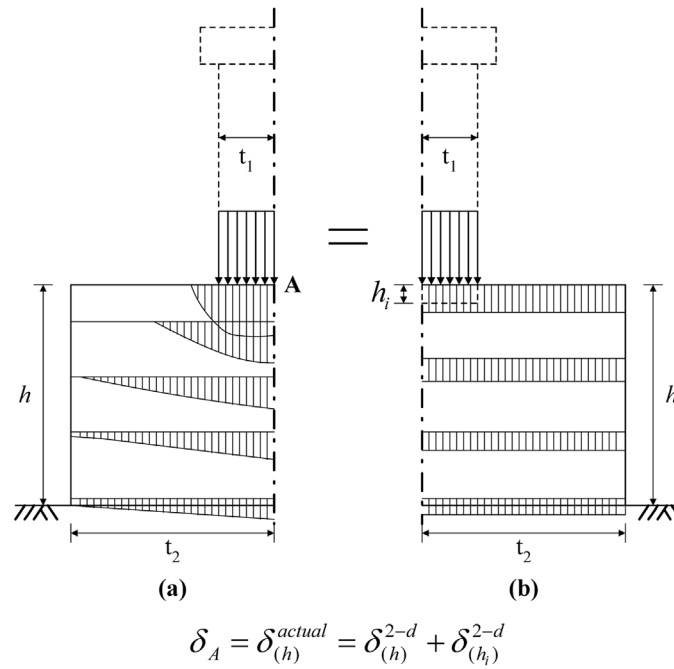
Fig. 7 Compressive stress distribution in plane between two different elements assumed for three-dimensional effect: (a) actual distribution; (b) two-dimensional analysis

plastic strain of reinforcing bars is an important variable of low cycle fatigue. This study applied the Coffin-Manson equation (Mander, *et al.* 1994), which is modified so that it can be applied to reinforced concrete (Kim, *et al.* 2005).

2.2. Confinement in concrete by reinforcements

The transverse reinforcements confine the compressed concrete in the core region and inhibit the buckling of the longitudinal reinforcing bars. In addition, the reinforcements also improve the ductility capacity of the unconfined concrete (Mander, *et al.* 1988).

This study basically adopted models proposed by Mander, *et al.* (1988) and Sun and Sakino (2000). The models consider the yield strength, the distribution type and the amount of the longitudinal and transverse reinforcing bars to compute the effective lateral confining stress and the ultimate compressive strength and strain of the confined concrete.

This study adopted the model proposed by Mander, *et al.* (1988) for normal strength concrete of below 30 MPa and adopted the model proposed by Sun and Sakino (2000) for high strength concrete of above 40 MPa. Because of the model proposed by Mander, *et al.* (1988) tends to overestimate the confinement effects when concrete strength becomes higher than 30 MPa and the model proposed by Sun and Sakino (2000) tends to underestimate the confinement effects when concrete strength becomes lower than 40 MPa. An analytical model was proposed for confined intermediate strength concrete from 30 MPa to 40 MPa. It was developed by modifying the earlier model proposed by Mander, *et al.* (1988) for normal strength concrete and Sun and Sakino (2000) for high strength concrete. The model incorporates all relevant parameters of confinement with a

smooth transition from 30 MPa to 40 MPa.

The stress-strain relationship for confined concrete is given by

$$\frac{f'_{cc}}{f'_{co}} = -1.254 + 2.254\sqrt{1+\frac{7.94f'_l}{f'_{co}}} - 2\frac{f'_l}{f'_{co}} = sk_{Mander} \quad \text{for} \quad f'_{co} \leq 30 \text{ MPa} \tag{1}$$

$$\frac{f'_{cc}}{f'_{co}} = 1 + 2.05\frac{\rho_s f_{yh}}{f'_{co}}\left(1-\frac{s}{2d_c}\right)^2 = sk_{Sun\&Sakino} \quad \text{for} \quad f'_{co} > 40 \text{ MPa} \tag{2}$$

$$\frac{f'_{cc}}{f'_{co}} = \frac{(f'_{co}-30)}{10}sk_{Sun\&Sakino} + \frac{(40-f'_{co})}{10}sk_{Mander} \quad \text{for} \quad 30 \text{ MPa} < f'_{co} \leq 40 \text{ MPa} \tag{3}$$

$$\frac{\varepsilon_{cc}}{\varepsilon_{co}} = 1 + 5\left(\frac{f'_{cc}}{f'_{co}}-1\right) = nk_{Mander} \quad \text{for} \quad f'_{co} \leq 30 \text{ MPa} \tag{4}$$

$$\frac{\varepsilon_{cc}}{\varepsilon_{co}} = \begin{cases} 1+4.7\left(\frac{f'_{cc}}{f'_{co}}-1\right), \frac{f'_{cc}}{f'_{co}} \leq 1.5 \\ \\ 3.35+20\left(\frac{f'_{cc}}{f'_{co}}-1.5\right), \frac{f'_{cc}}{f'_{co}} > 1.5 \end{cases} = nk_{Sun\&Sakino} \quad \text{for} \quad f'_{co} > 40 \text{ MPa} \tag{5}$$

$$\frac{\varepsilon_{co}}{\varepsilon_{co}} = \frac{(f'_{co}-30)}{10}nk_{Sun\&Sakino} + \frac{(40-f'_{co})}{10}nk_{Mander} \quad \text{for} \quad 30 \text{ MPa} < f'_{co} \leq 40 \text{ MPa} \tag{6}$$

where f'_{cc} = confined concrete compressive strength; f'_{co} = unconfined concrete compressive strength; f'_l = effective lateral confining stress; ρ_s = volumetric ratio of the confining steel; f_{yh} = yield strength of the confining steel; s = pitch of confining steel; d_c = diameter of confining steel between bar center; sk = confining parameter of strength; ε_{cc} = peak strain of confined concrete; ε_{co} = peak strain of unconfined concrete; nk = confining parameter of strain.

3. Model for unbonded reinforcing or prestressing bars

For bonded bars, the deformation field of the bar is the same as that of the concrete on the interface. However, in the case of unbonded bars, including bonded post-tensioned structures in the prestressing transfer stage, the deformation field of the bar is not equal to that of the concrete, except at the anchorage. Complex iterative procedures are needed to satisfy the displacement compatibility between concrete and unbonded bar at the anchorage because of interactions between concrete and unbonded bars. To represent the interaction between the concrete and unbonded bar, the contribution of the unbonded bar is represented by equivalent loads.

In this study, a numerical model for discretized unbonded reinforcing or prestressing bars is proposed based on the finite element method, which can represent the interaction between the unbonded bar and concrete. This model can be used to efficiently represent the transfer processes for unbonded bars.
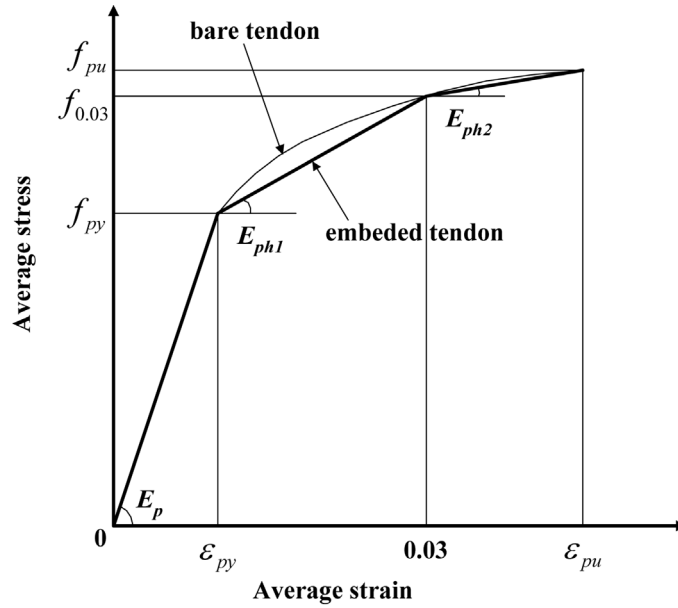
Fig. 8 Model for unbonded prestressing bar

3.1. Nonlinear material model for unbonded prestressing bars

Bilinear diagrams used to characterize the mild steel behavior of brusque yielding cannot be immediately extrapolated to unbonded prestressing bar. For unbonded prestressing bars, which does not have a definite yield point a multilinear approximation may be required. In this study, the modified modeling is adopted for the present formulation as follows (see Fig. 8). A trilinear model for the stress-strain relationship of unbonded prestressing bar considering the bond effect has been used. Unloading and reloading processes are accounted for through straight branches with an initial modulus.

$$\sigma_{pt} = f_{py} + E_{ph1}(0.03 - \varepsilon_{py}) + E_{ph2}(\varepsilon_{pu} - 0.03) \tag{7}$$

$$E_{ph1} = \frac{f_{0.03} - f_{py}}{0.03 - \varepsilon_{py}} \tag{8}$$

$$E_{ph2} = \frac{f_{pu} - f_{0.03}}{\varepsilon_{pu} - 0.03} \tag{9}$$

where σ_{pt} = stress of unbonded prestressing bars; f_{py} = yielding strength of unbonded prestressing bars; f_{pu} = ultimate strength of unbonded prestressing bars; ε_{py} = yielding strain of unbonded prestressing bars; ε_{pu} = ultimate strain of unbonded prestressing bars; and E_{ph1}, E_{ph2} = strain hardening rates of the unbonded prestressing bars embedded in concrete.

3.2. Formulation for unbonded reinforcing or prestressing bars

An essential feature built into the program was the modeling of unbonded reinforcing or prestressing bar behavior. The modeling is based on analysis method for internal unbonded post-

tensioned beams proposed by Harajli (1990). This method is similar to that for bonded bars, but the stress in the unbonded bars cannot be evaluated from force equilibrium and strain compatibility alone, since the assumption of prefect bond between the bars and the concrete is no longer valid along the unbonded regions. Instead, the change in stress in the unbonded bars for any given loading depends on the average change in stress in the adjacent concrete all over the unbonded length of the bars.

The strain in unbonded bars is not compatible with that of the adjacent concrete over the unbonded length l_u. The average increase in strain in this unbonded bar, along its unbonded length, is then

$$\Delta\varepsilon_s = \frac{\Delta l_s}{l_u} \tag{10}$$

where Δl_s = total elongation of the unbonded bars.

The total strain ε_s is determined by

$$\varepsilon_s = \varepsilon_{pe} + \Delta\varepsilon_s \tag{11}$$

where ε_{pe} = effective pre-strain in the unbonded bars.

The corresponding stress in the unbonded bars is obtained from the previous section stress-strain curve, whereas the stress in the bonded bars is found by the conventional strain compatibility method.

Highly iterative procedure is required to analyze the regions of unbonded bars. The analysis of unbonded bars was also found to be susceptible to convergence problems and some considerable effort was spent in developing program methodologies to provide efficient solutions.

4. Reinforced concrete bridge piers with unbonded reinforcing bars

4.1. Description of test specimens

Three reinforced concrete specimens were loaded to evaluate the effect of unbonding of longitudinal reinforcements at the plastic hinge region on the enhancement of the ductility of

Table 1 Test specimens (Kawashima, *et al.* 2001)

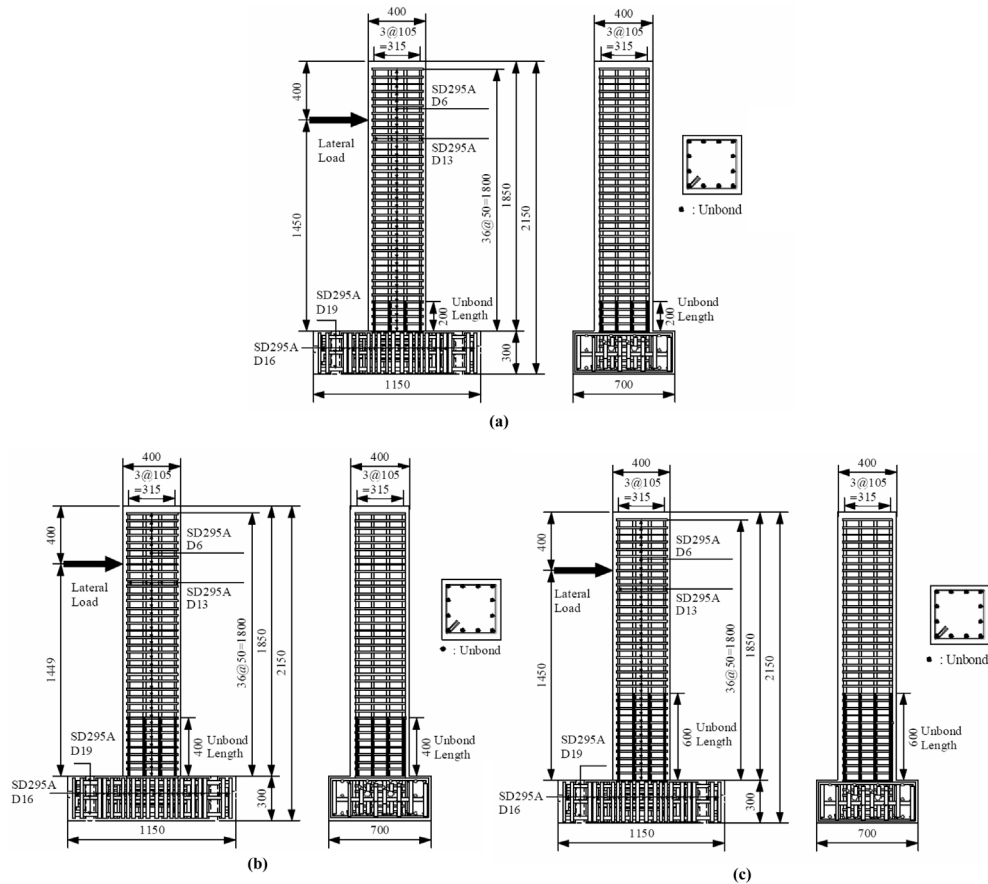| Item	TP-14	TP-15	TP-16
Section		Square	
Section size (mm)		400×400	
Effective height (mm)		1450	
Effective depth (mm)		360	
Aspect ratio		4.03	
Longitudinal reinforcement ratio (%)		0.95	
Volumetric ratio of tie reinforcement (%)		0.77	
Cylinder strength of concrete (MPa)	23.6	24.6	23.5
Longitudinal reinforcement		SD295A D13 (Yield strength = 367 MPa)	
Tie reinforcement		SD295A D6 (Yield strength = 376 MPa)	
Axial force		160 kN(1.05 MPa at the bottom)	

Fig. 9 Test specimens (Unit: mm) (Kawashima, *et al*. 2001): (a) TP-14; (b) TP-15; (c) TP-16

reinforced concrete bridge piers (Kawashima, *et al*. 2001). Table 1 shows the specifications of the specimens. Fig. 9 and 10 show the size and reinforcements.

Three 400×400 mm square reinforced concrete bridge piers were tested under reversed cyclic loading. The bridge piers were cyclically loaded 3 times at each loading displacement δ_y, $2\delta_y$, $3\delta_y$, …, until failure.

A poor bond condition was achieved by replacing deformed bars by round bars with plastic materials on the surface. By appropriately unbonding the longitudinal bars between an interval with unbonded length as shown in Fig. 9, the deformation of the longitudinal bars is reduced by avoiding the concentration of strain.

4.2. Description of analytical model

Fig. 11 shows the finite element discretization and the boundary conditions for two-dimensional plane stress nonlinear analyses of the reinforced concrete bridge piers. The interface element between the footing and the column enhanced the effects of the bond-slip of steel bars and the local compression. The unbonded bar element was also used to describe the inelastic behaviors of unbonded reinforcing bars.

Loading cycles with displacement control were applied as this allows the analysis beyond the ultimate load where the load at the maximum strain was recognized from the load displacement curve.
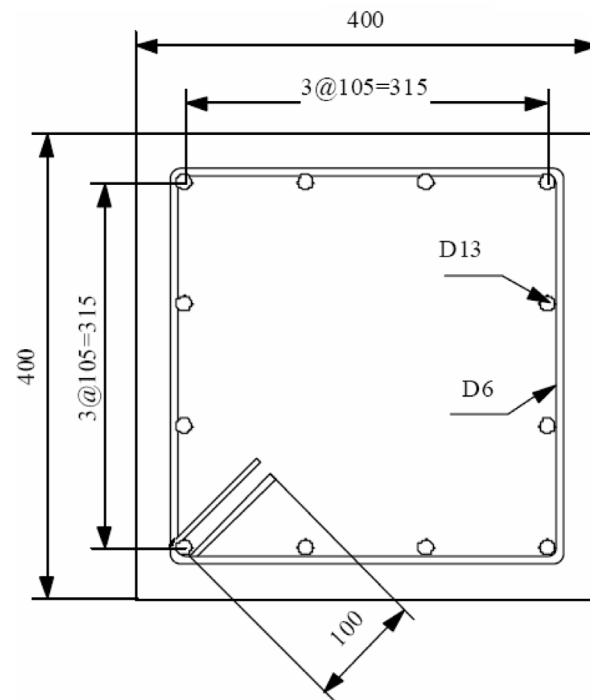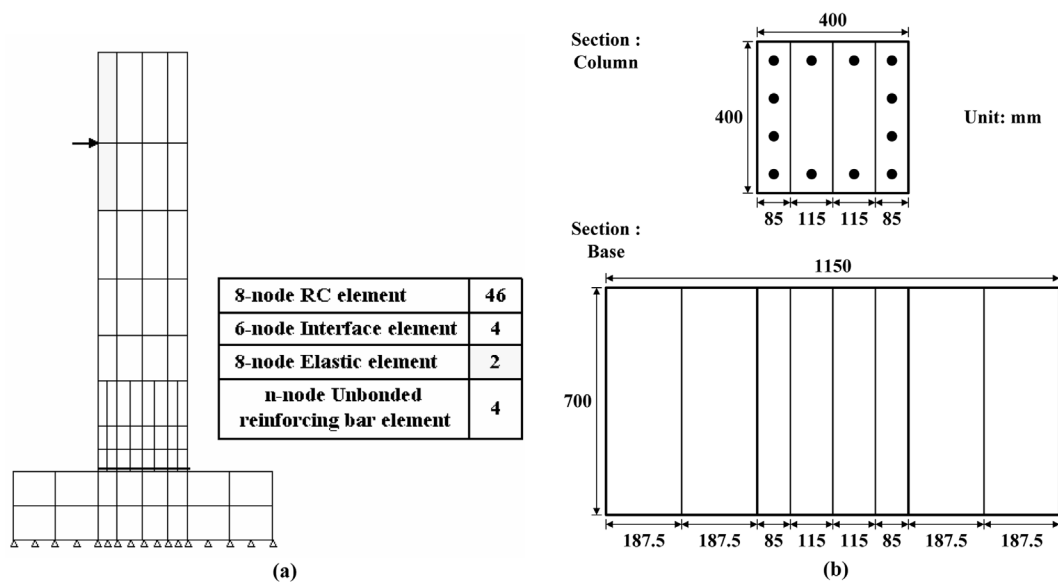
Fig. 10 Cross section (Unit: mm) (Kawashima, *et al.* 2001)

Fig. 11 The finite element mesh for the analysis: (a) finite element model; (b) cross section for using plane stress elements

4.3. Comparison with experimental results

Fig. 12 compares the lateral force versus lateral displacement hystereses. The analytical results showed reasonable correspondence with experimental results (Kim and Shin 2005).

The restoring force of the TP-14 starts to deteriorate at $10\delta_y$, while the restoring force is stable until $12\delta_y$ in the TP-15 and TP-16. In comparison, the failure of concrete was much less in the unbonded column for a smaller unbonded length. The unbonded bridge piers showed large displacement response. The stiffness reduced slightly because of the unbonding but ductility increased remarkably. The ductility of the unbonded specimen improved remarkably with a very little reduction in stiffness and delay in yielding.

An important feature of the unbonded column is the rocking response of the column relative to the footing. Since the longitudinal bars are unbonded for a length, the longitudinal bars in tension pull out from the column, which results in a dominant rocking response of the column.

Based on the experimental and analytical studies, it is considered that the unbonding is an effective means to increase the ductility capacity of columns when the unbonded length is chosen properly. Experimental and analytical results showed that this method was very effective in completely altering the failure mode at the ultimate state from shear to flexure. This method was also found to produce remarkable improvement in the ductility of reinforced concrete bridge piers. The unbonded bridge piers showed larger seismic displacement than ordinary reinforced concrete bridge piers did because of the smaller amount of energy absorption.
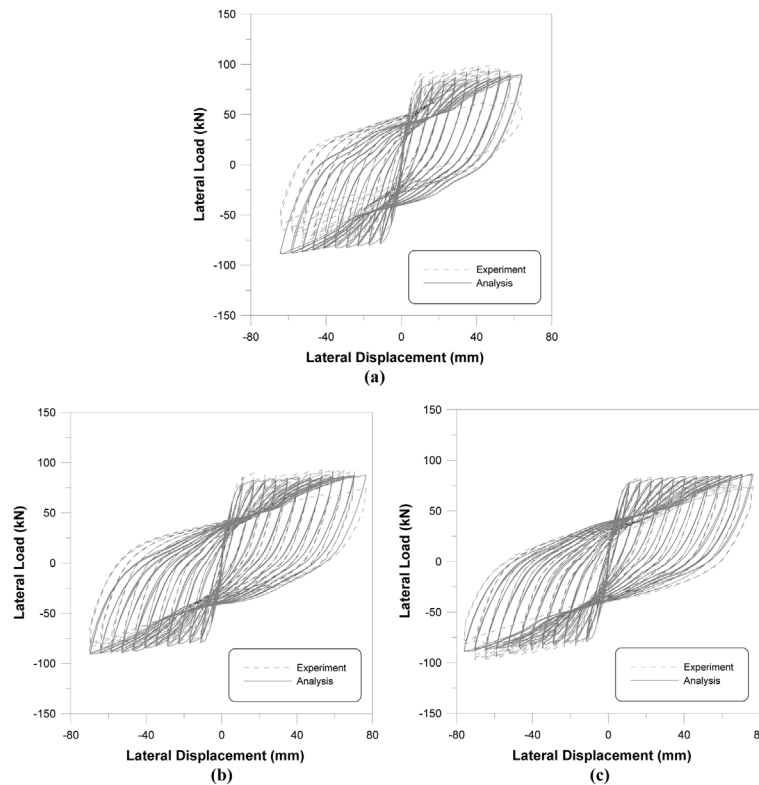

Fig. 12 Hysteresis loop for specimens: (a) TP-14; (b) TP-15; (c) TP-16

5. Reinforced concrete bridge piers with unbonded prestressing bars

5.1. Description of test specimens

In the loading test, rectangular reinforced concrete bridge piers with unbonded prestressing bars with an effective height of 1.0 m and a section of 300 mm by 300 mm were constructed. The axial force and prestress were studied as parameters. To clarify the effect of tensioning level on the behavior of reinforced concrete bridge piers with unbonded prestressing bars, test was conducted with specimens having different tensioning level (Ito, *et al.* 1997). The bridge piers were subjected to an axial load (dead load of the superstructure) equivalent to 10 kgf/cm^2 (0.98 MPa) or 40 kgf/cm^2 (3.92 MPa), and the prestress was either 35 kgf/cm^2 (3.43 MPa) or 70 kgf/cm^2 (6.86 MPa). The hysteresis of a standard reinforced concrete bridge pier is also presented here for comparison.
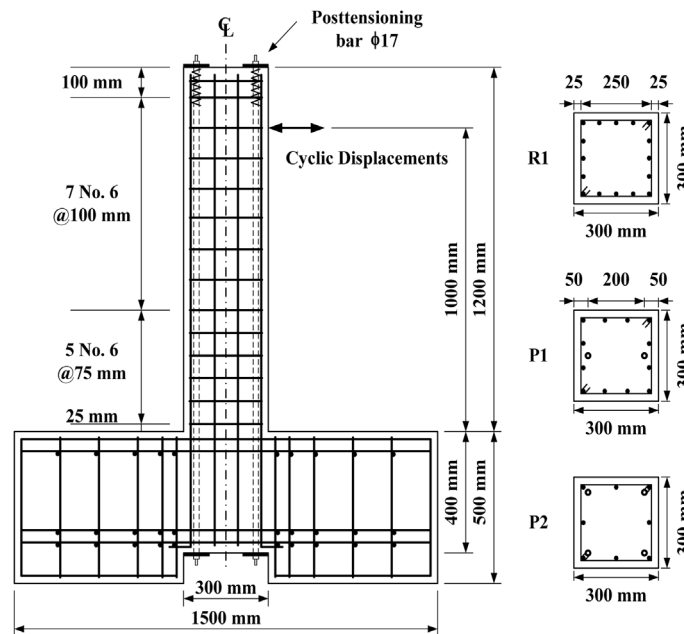

Fig. 13 Test specimens (Ito *et al.* 1997)

Table 2 Test specimens (Ito, *et al.* 1997)

Specimen	Axial force (kgf/cm^2)	f_c (kgf/cm^2)	Mild steel	Mild steel f_y (kgf/cm^2)	Prestress steel (f_y= 12,500 kgf/cm^2)	Prestress (kgf/cm^2)	Shear reinf. (f_y= 3,540 kgf/cm^2)
R1(N)	10	356	16-D13	3,880	-	0	Base: D6@75 mm; Elsewhere: D6@100 mm
P1(N)			12-D10	4,090	2-Φ17 mm	35	
P2(N)			8-D6	3,540	4-Φ17 mm	70	
R1(H)	40		16-D13	3,880	-	0	
P1(H)			12-D10	4,090	2-Φ17 mm	35	
P2(H)			8-D6	3,540	4-Φ17 mm	70	

Note: 1 kgf/cm^2 = 0.098 MPa

The elevation and cross sections of the test specimens are shown in Fig. 13. The geometry and material properties of the columns are summarized in Table 2. The specimens were subjected to an external axial stress and displacement cycles in multiples of the yield displacements.

5.2. Description of analytical model

Fig. 14 shows the finite element discretization and the boundary conditions for a sample of
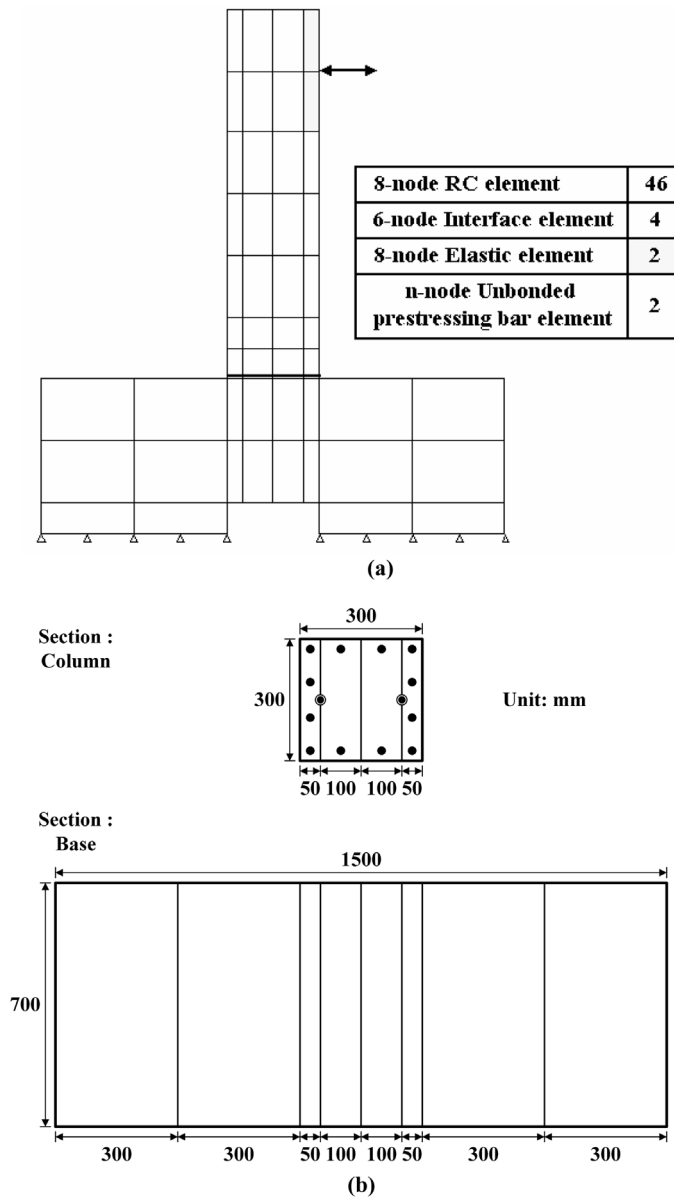
8-node RC element	46
6-node Interface element	4
8-node Elastic element	2
n-node Unbonded prestressing bar element	2

(a)

Section : Column

300

300

Unit: mm

50 100 100 50

Section : Base

1500

700

300   300   50 100 100 50   300   300

(b)

Fig. 14 The finite element mesh for the analysis (specimen P1): (a) finite element model; (b) cross section for using plane stress elements

specimens, and the finite element model consists of eight-noded plane stress elements. The unbonded prestressing bars are modeled with developed unbonded bar element.

Effective prestress was applied in the unbonded prestressing bar, and the external axial load was applied as a distributed force at the top of the bridge pier. Cyclic lateral displacement was then applied as in the experiment.

5.3. Comparison with experimental results

Figs. 15 through 20 show a comparison between the experimental and analytical behavior for this test. The analytical results showed reasonable correspondence with the experimental results (Kim *et al.* 2005).

The analytical model was accurate and reliable overall in predicting the structural response of reinforced concrete bridge piers with unbonded prestressing bars.

If one defines the unload residual displacement as a residual lateral displacement of a bridge pier when the lateral force is equal to zero after unloaded from a maximum lateral displacement, then the unloaded residual displacement is significantly smaller in the reinforced concrete bridge piers with unbonded prestressing bars than in the standard reinforced concrete bridge piers. It is obvious from a nonlinear behavior response analysis that the limited unloaded residual displacement contributes to the reduction of the residual displacement of a bridge pier after an extreme earthquake.

In the experiments, unbonded prestressing decreased the energy dissipation capacity and residual displacements. These effects were also observed in the simulations. The accumulated energy absorption decreased as the level of prestress increased, and this tendency did not largely vary with the displacement. And also the residual displacement decreased in the same way, but the residual displacement of the specimens prestressed by 35 kgf/cm^2 (3.43 MPa) and 70 kgf/cm^2 (6.86 MPa) did not change significantly.

Pinching effect was clearly visible in the load displacement curves. This effect was attributed to the occurrence of wide diagonal shear crack with the load reversal in P1 and P2. On the other hand,
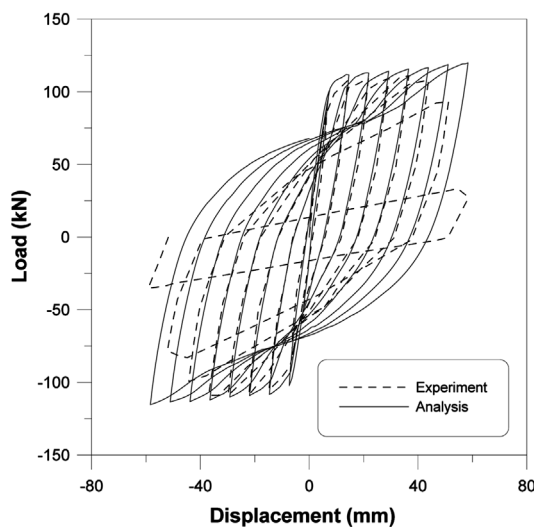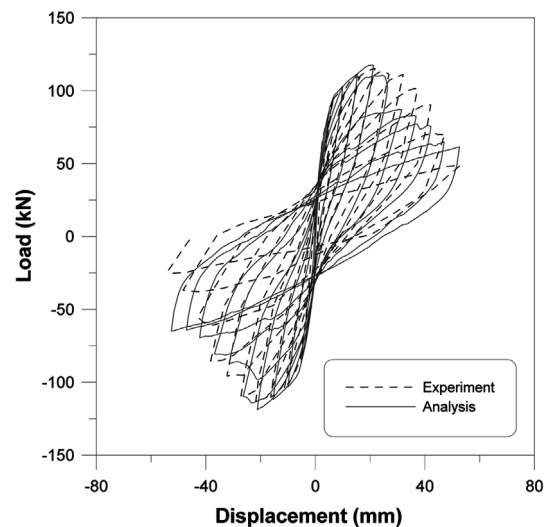

Fig. 15 Hysteresis loop for specimen R1(N)

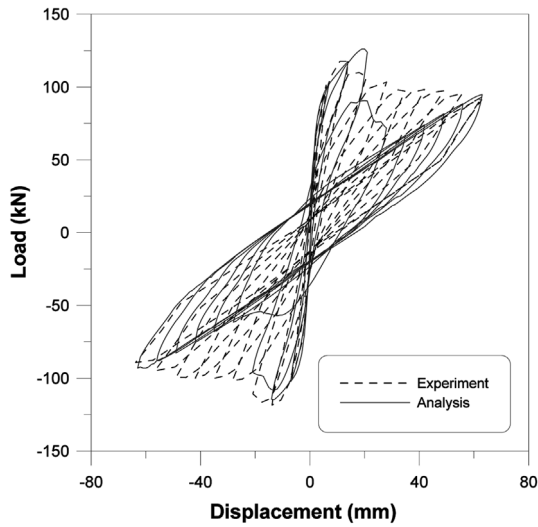Fig. 16 Hysteresis loop for specimen P1(N)

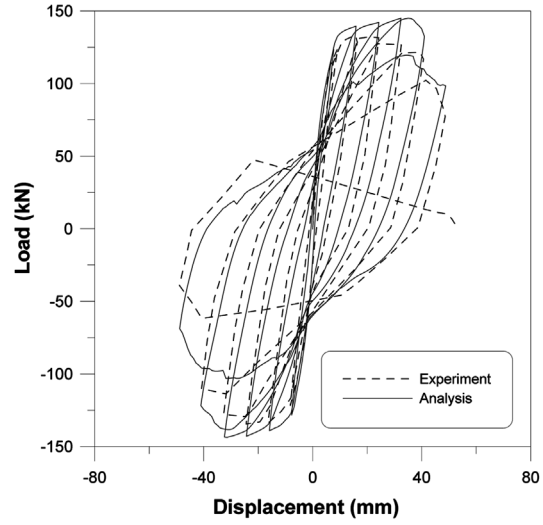Fig. 17 Hysteresis loop for specimen P2(N)

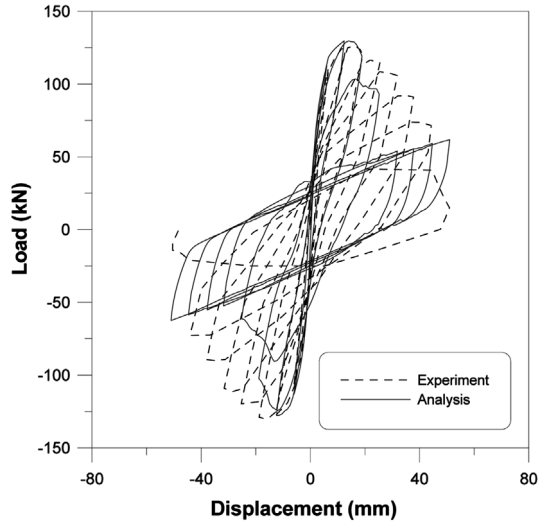Fig. 18 Hysteresis loop for specimen R1(H)
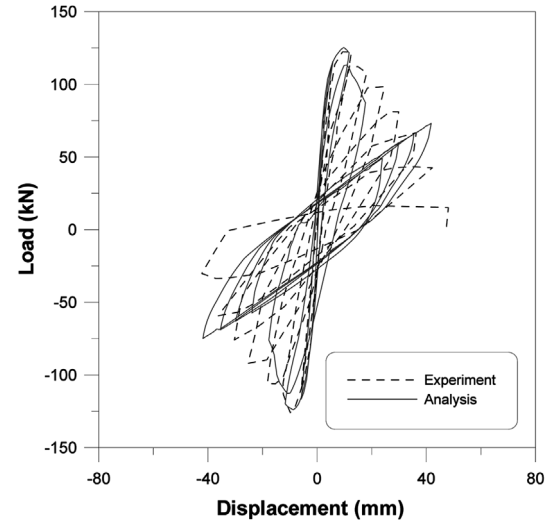

Fig. 19 Hysteresis loop for specimen P1(H)

Fig. 20 Hysteresis loop for specimen P2(H)

pinching in unbonded specimens was due to the occurrence of large flexural crack at the column-footing joint.

The deformation capacity was improved with the level of prestress. On the other hand, increase of the axial stress by the external axial force and the prestress decreased the ductility ratio, as shown in Fig. 21. Fig. 22 shows the damage pattern of the specimens at failure. Damage was concentrated only at the column-footing joint. The calculated failure sequence was in good agreement with the tested failure sequence. The final failure was due to the crushing of concrete, followed by the yielding of the longitudinal bars.
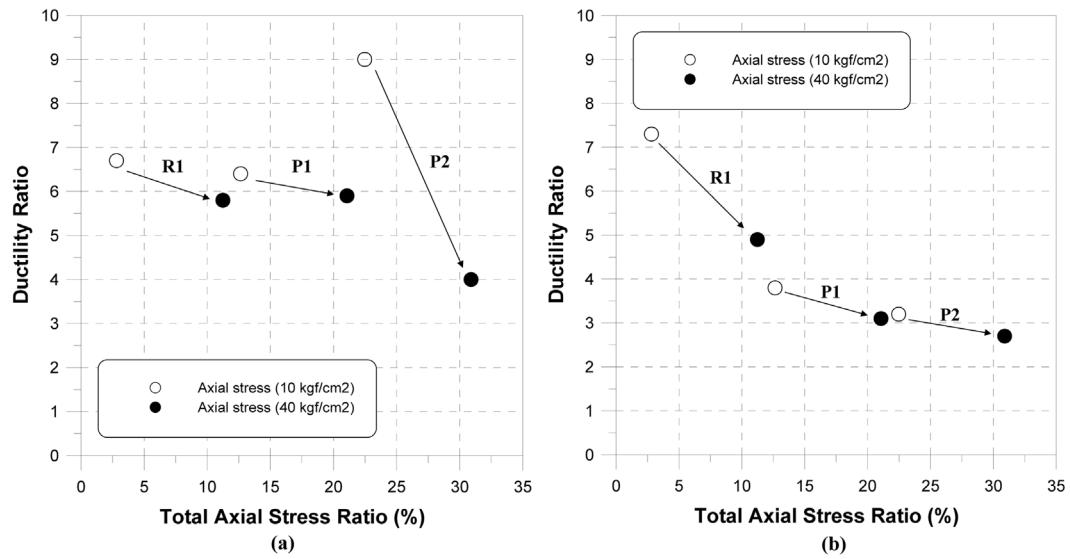
Fig. 21 Ductility ratio for total axial stress ratio: (a) Experiment; (b) Analysis (1 kgf/cm^2 = 0.098 MPa)
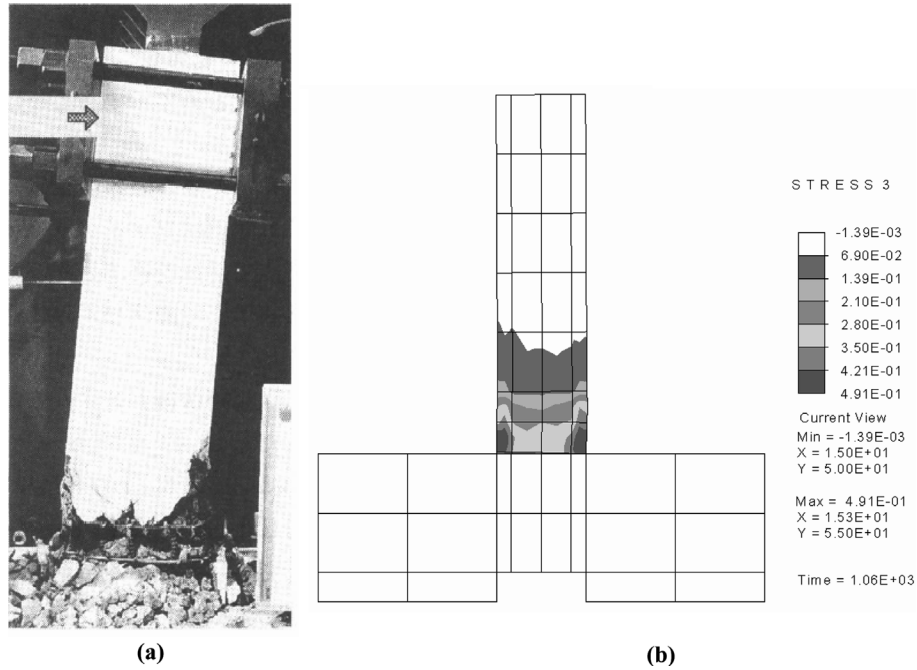

Fig. 22 Failure mode for specimen R1(N) : (a) Experiment; (b) Analysis

6. Conclusions

This paper presents a new method for the nonlinear analysis of reinforced concrete bridge piers with unbonded reinforcing or prestressing bars. Theory and formulations for analytical models to be

implemented with numerical methods for predicting the behavior of reinforced concrete bridge piers with unbonded bars are described. The agreement between the numerical results and experimental results demonstrate the overall accuracy and reliability of the analytical models in predicting the response of reinforced concrete bridge piers with unbonded bars. It is expected that, by using the proposed models, the seismic response of reinforced concrete bridge piers with unbonded reinforcing or prestressing bars can be predicted accurately so that bridge piers can be designed more rationally and reliably. From the results of the numerical simulations and comparisons with experimental results, the following conclusions are reached.

1. The material models used for modeling concrete and reinforcing bars in this study gave promising results for the seismic performance assessment of the reinforced concrete bridge piers with unbonded bars.
2. Unbonding of longitudinal bar can completely change the failure mode of the bridge piers at the ultimate state from shear to flexure and it remarkably increases the ductility.
3. The influence of vertical prestressing in a bridge pier, which reduces the energy dissipation capacity and the residual displacement, can be successfully predicted.
4. By using proposed numerical method to study the seismic response of reinforced concrete bridge piers with unbonded bars, one can design more realistic and safe bridge piers.
5. Further efforts should be directed to include certain procedures in the current design codes to direct the engineers toward an acceptable method for evaluating the available strength in existing reinforced concrete bridge piers.

Acknowledgements

References

Chung, Y.-S., Park, C.-K. and Lee, E.-H. (2004), "Seismic performance and damage assessment of reinforced concrete bridge piers with lap-spliced longitudinal steels", *Struct. Eng. Mech.*, **17**(1), 99-112.

Harajli, M. H. (1990), "Effect of span-depth ratio on the ultimate steel stress in unbonded prestressed concrete members", *ACI Struct. J.*, **87**(3), 305-312.

Ikeda, S., Hirose, S., Yamaguchi, T., and Nonaka, S. (2002), "Seismic performance of concrete piers prestressed in the critical section", *The First Fib Congress*, CD.

Ito, T., Yamaguchi, T. and Ikeda, S. (1997), "Seismic performance of reinforced concrete piers prestressed in axial directon", *Proc., JCI*, **19**(2), 1197-1202 (in Japanese).

Kakuta, Y., Okamura, H. and Kohno, M. (1982), "New concepts for concrete fatigue design procedures in Japan", *IABSE Colloquium of Fatigue of Steel and Concrete Structures*, Lausanne, 51-58.

Kato, B. (1979), "Mechanical properties of steel under load cycles idealizing seismic action", *CEB Bulletin D'Information*, **131**, 7-27.

Kawashima, K., Hosoiri, K., Shoji, G. and Sakai, J. (2001), "Effect of unbonding of main reinforcements at plastic hinge region for enhanced ductility of reinforced concrete bridge columns", *Proc., JSCE*, **689**(I-57), 45-64, (in Japanese).

Kwan, W.-P. and Billington, S. L. (2001), "Simulation of structural concrete under cyclic load", *J. Struct. Eng., ASCE*, **127**(12), 1391-1401.

Kim, T.-H., Lee, K.-M., Chung, Y.-S. and Shin, H. M. (2005), "Seismic damage assessment of reinforced concrete bridge columns", *Eng. Struct.*, **27**(4), 576-592.

Kim, T.-H., Lee, K.-M. and Shin, H. M. (2002), "Nonlinear analysis of reinforced concrete shells using layered elements with drilling degree of freedom", *ACI Struct. J.*, **99**(4), 418-426.

Kim, T.-H., Lee, K.-M., Yoon, C.-Y. and Shin, H. M. (2003), "Inelastic behavior and ductility capacity of reinforced concrete bridge piers under earthquake. I: theory and formulation", *J. Struct. Eng., ASCE*, **129**(9), 1199-1207.

Kim, T.-H., Park, J.-G., Jin, B.-M. and Shin, H. M. (2005), "Analytical study on the inelastic behavior of reinforced concrete bridge columns with unbonded tendons", *Journal of the Korean Society of Civil Engineers, KSCE,* **25**(5A), 813-821, (in Korean).

Kim, T.-H. and Shin, H. M. (2001), "Analytical approach to evaluate the inelastic behaviors of reinforced concrete structures under seismic loads", *Journal of the Earthquake Engineering Society of Korea*, EESK, **5**(2), 113-124.

Kim, T.-H. and Shin, H. M. (2005), "Analytical study on inelastic behavior of RC bridge columns with unbonding of main reinforcements at plastic hinge region", *Journal of the Earthquake Engineering Society of Korea*, *EESK*, **9**(2), 29-36, (in Korean).

Li, B., Maekawa, K. and Okamura, H. (1989), "Contact density model for stress transfer across cracks in concrete", *Journal of the Faculty of Engineering*, University of Tokyo (B), **40**(1), 9-52.

Maekawa, K., and Okamura, H. (1983), "The deformational behavior and constitutive equation of concrete using elasto-plastic and fracture model", *Journal of the Faculty of Engineering*, University of Tokyo (B), **37**(2), 253-328.

Mander, J. B., Panthaki, F. D. and Kasalanati, K. (1994), "Low-cycle fatigue behavior of reinforcing steel", *J. Mater. Civ. Eng.*, *ASCE*, **6**(4), 453-468.

Mander, J. B., Priestley, M. J. N. and Park, R. (1988), "Theoretical stress-strain model for confined concrete", *J. Struct. Eng.*, *ASCE*, **114**(8), 1804-1826.

Mori, T., Park, D. K., Ikeda, S. and Yoshioka, T. (2002), "Seismic performance of prestressed concrete piers", *The First Fib Congress*, CD.

Mutsuyoshi, H., Zatar, W. A. and Maki, T. (2001), "Seismic behavior of partially prestressed concrete piers", *Proc.*, *JSCE*, **669**(V-50), 27-38.

Pandey, G. R. and Mutsuyoshi, H. (2004), "Seismic damage mitigation of reinforced concrete bridge piers by unbonding longitudinal reinforcements", *13th World Conference on Earthquake Engineering*, CD.

Ranasinghe, K., Mutsuyoshi, H., and Uchibori, H. (2002), "Cyclic testing of reinforced concrete columns with unbonded reinforcements", *Proc.*, *JCI*, **24**(2), 1141-1146.

Shima, H., Chou, L. and Okamura, H. (1987), "Micro and macro models for bond behavior in reinforced concrete", *Journal of the Faculty of Engineering*, University of Tokyo (B), **39**(2), 133-194.

Sun Y.-P. and Sakino, K. (2000), "A comprehensive stress-strain model for high strength concrete confined by circular transverse reinforcement", *The 6th ASCCS International Conference on Steel-Concrete Composite Structures*, University of Southern California, 1067-1074.

Taylor, R. L. (2000), *FEAP - A finite element analysis program*, version 7.2 users manual, volume 1 and volume 2, Department of Civil and Environmental Engineering, University of California at Berkeley.

CC